Surface Structure, Adsorption and Thermal Desorption Behaviors of Methaneselenolate Monolayers on Au (111) from Dimethyl Diselenides

ARTICLE *in* THE JOURNAL OF PHYSICAL CHEMISTRY C · APRIL 2014

Impact Factor: 4.77 · DOI: 10.1021/jp409531w

6 AUTHORS, INCLUDING:

Sang Yun Lee
Ulsan Techno Park
15 PUBLICATIONS **250** CITATIONS
SEE PROFILE

Haiwon Lee
Hanyang University
840 PUBLICATIONS **12,130** CITATIONS
SEE PROFILE

Jaegeun Noh
Hanyang University
105 PUBLICATIONS **1,733** CITATIONS
SEE PROFILE

THE JOURNAL OF PHYSICAL CHEMISTRY C

Article

pubs.acs.org/JPCC

Surface Structure, Adsorption, and Thermal Desorption Behaviors of Methaneselenolate Monolayers on Au(111) from Dimethyl Diselenides

Sang Yun Lee,*[,†,‡] Eisuke Ito,[‡] Hungu Kang,[§] Masahiko Hara,[‡,∥] Haiwon Lee,[†,§] and Jaegeun Noh*[,†,§]

[†]Institute of Nano Science and Technology and [§]Department of Chemistry, Hanyang University, 17 Haengdang-dong, Seongdong-gu, Seoul 133-791, Korea

[‡]Flucto-Order Functions Research Team, RIKEN-HYU Collaboration Research Center, RIKEN, 2-1 Hirosawa, Wako, Saitama 351-0198, Japan

[∥]Department of Electronic Chemistry, Tokyo Institute of Technology, 4259 Nagatsuta-cho, Midori-ku, Yokohama, Kanagawa 226-8503, Japan

Supporting Information

ABSTRACT: To understand the effect of headgroups (i.e., sulfur and selenium) on surface structure, adsorption states, and thermal desorption behaviors of self-assembled monolayers (SAMs) on Au(111), we examined methanethiolate (CH_3−S, MS) and metheneselenolate (CH_3−Se, MSe) monolayers formed from dimethyl disulfide (DMDS) and dimethyl diselenide (DMDSe) molecules by ambient vapor-phase deposition. Scanning tunneling microscopy imaging revealed that DMDS molecules on Au(111) after a 1 h deposition form MS monolayers containing a disordered phase and an ordered row phase with an inter-row spacing of 1.51 nm, whereas DMDSe molecules form long-range-ordered MSe monolayers with a $(\sqrt{3} \times 3\sqrt{3})R30°$ structure. X-ray photoelectron spectroscopy measurements showed that MS or MSe monolayers chemisorbed on Au(111) were formed via S−S bond cleavage of DMDS or Se−Se bond cleavage of DMDSe. On the other hand, we monitored three main desorption fragments for MS and MSe monolayers using TDS monomers (CH_3S^+, CH_3Se^+), parent mass species (CH_3SH^+, CH_3SeH^+), and dimers (CH_3S−SCH_3^+, CH_3Se−$SeCH_3^+$). Interestingly, we found that thermal desorption behaviors of MSe monolayers were markedly different from those of MS monolayers. All desorption peaks for MSe monolayers were observed at a higher temperature compared with MS monolayers, suggesting that the adsorption affinity of selenium atoms for the Au(111) surface is stronger than that of sulfur atoms. In addition, the desorption intensity of dimer fragments for MSe monolayers was much lower than for MS monolayers, indicating that selenolate SAMs on Au(111) did not undergo their dimerization efficiently during thermal heating compared with thiolate SAMs. Our results provide new insight into understanding the surface structure and thermal desorption behavior of MSe monolayers on Au(111) surface by comparing those of MS monolayers.

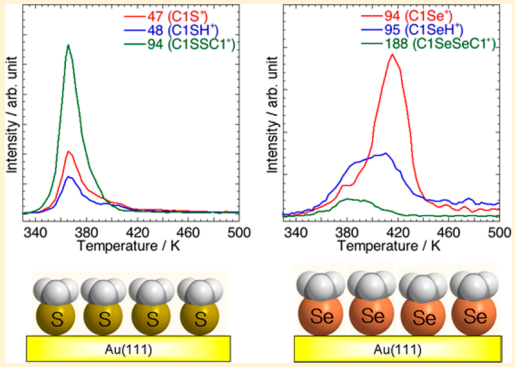

INTRODUCTION

Over recent decades, self-assembled monolayers (SAMs) have gained interest for nanoscience and nanotechnologies, such as electronic devices, sensors, and nanolithography.[1−9] In particular, thiol SAMs on metal surfaces have been widely studied due to their advantages such as chemical stability, superior reproducibility, and functional tunability.[3,5,8,10−20] Despite their amenability to various characterizations, thiol SAMs are susceptible to oxidization, resulting in the formation of disulfides and other species during SAM preparation.[21−23] To alleviate this difficulty, other sulfur-containing precursors such as thiosulfates,[24] acetyl-functioned thiols,[25] and thiocyanates[26−31] have been investigated as alternatives for thiolate assemblies. Extended to other headgroups, selenium has attracted particular attention, since it belongs to the same group as sulfur in the periodic table, group 16. Despite the published values for headgroup interactions with surfaces,[32] experimental studies have exhibited contradictory results, since the bond energy difference between selenium and sulfur toward metal surfaces is negligible enough to be influenced by other effects.[33−47] Among the controversies, it was recently proposed that selenium has a higher affinity toward gold surfaces compared to sulfur on the basis of theoretical calculation.[36,47] Meanwhile, organoselenium SAMs on noble metals have been investigated as alternative assemblies.[48] Previously, scanning tunneling microscopy (STM) studies revealed that benzeneselenols and diphenyl diselenide SAMs can form various ordered structures on Au(111) such as $(3\sqrt{3} \times 2\sqrt{3})R30°$ or $(4\sqrt{3} \times$

Received: September 24, 2013
Revised: March 17, 2014
Published: March 22, 2014

   dx.doi.org/10.1021/jp409531w | J. Phys. Chem. C 2014, 118, 8322−8330

$2\sqrt{3})R30°$ with a low molecular packing density.[37,49] Similarly, docosaneselenol and decaneselenol were shown to form stable SAMs on Au(111) surfaces in a manner analogous to that of alkanethiol SAMs.[41,50] Choi et al. reported that octaneselenolate (OSe) SAMs form long-range ordered structures with a $(6 \times \sqrt{3})R30°$ superlattice rather than the $(\sqrt{3} \times \sqrt{3})R30°$ or $c(2 \times 4)$ structures typical of alkanethiol SAMs. Contrary to octanethiol SAMs, OSe SAMs form ordered structures with a shorter immersion time and at a lower solution concentration.[34,35] Conversely, a study employing reflection absorption infrared spectroscopy suggested that adoption of neat diselenide is essential to obtain highly ordered structures for SAM formation.[51] On the other hand, solvent molecules in diluted solution deposition prevent molecular ordering of SAMs formed by dihexyl diselenides with a shorter alkyl chain compared with didodecyl diselenides with a longer alkyl chain.[51] In addition, it has been suggested that the formation and structure of SAMs by organoselenium compounds is significantly influenced by preparation conditions and molecular backbone structures with different length alkyl chains, unlike organosulfur compounds. To the best of our knowledge, there have been no reports to date on the formation, surface structure, and thermal desorption behaviors of SAMs prepared by dialkyl diselenides with very short alkyl chains such as methyl or ethyl groups. These dialkyl diselenides are less susceptible to molecule-to-molecule interactions and thus should be primarily associated with headgroup-to-surface interactions.

In this study, to understand the effect of headgroups (sulfur and selenium) on the formation of SAMs on Au(111), we examined the surface structures, adsorption states, and thermal desorption behavior of methaneselenolate (CH_3−Se, MSe) monolayers from dimethyl diselenide (DMDSe) on Au(111) using STM, X-ray photoelectron spectroscopy (XPS), and thermal desorption spectroscopy (TDS). We compared these results with those of methanethiolate (CH_3−S, MS) monolayers with identical as well as short alkyl chains (i.e., methyl groups). Here, we report for the first time that MSe monolayers on Au(111) have a $(\sqrt{3} \times 3\sqrt{3})R30°$ packing structure and that the thermal stability and desorption behavior of MSe monolayers are significantly different from those of MS monolayers.

EXPERIMENTAL SECTION

Chemicals and Materials. Dimethyl disulfide (DMDS) and DMDSe were purchased from Sigma−Aldrich Co. LLC. (USA) and were used without further purification. (Caution! DMDSe is toxic and should be handled in fume hoods.) Ethanol of reagent grade was used as purchased from Daejung Chemicals Co., Ltd. (Korea). Au(111) substrates were prepared by vacuum deposition of gold onto freshly cleaved mica sheets prebaked at 623 K under a vacuum pressure of $\sim 10^{-5}$ to 10^{-6} Pa. After deposition, substrates were annealed at 623 K in the same vacuum chamber for 2 h. STM measurements showed that gold substrates contained atomically flat large terraces with herringbone reconstruction structures.

SAM Preparation. MS and MSe monolayers were prepared by placing a gold substrate in a V-vial containing 1 μL of corresponding neat liquids at 323 K for different deposition times of 1, 2, and 24 h (ambient-pressure vapor phase deposition). After deposition, the resulting monolayer samples were rinsed thoroughly with pure ethanol to remove the physisorbed molecules from the surface and dried with a high-purity N_2 gas stream.

STM, XPS, and TDS Measurements. STM measurements were performed using a NanoScope IIIa (Veeco Instruments Inc., USA) with a commercial Pt/Ir (80/20) tip. All STM images were obtained using constant current mode under ambient conditions at room temperature (296 K). Imaging conditions of bias voltage and tunneling current for all samples were 500 mV and 300 pA, respectively. XPS measurements were conducted using a Theta Probe (Thermo Fisher Scientific, UK). Monochromated Al Kα radiation (1486.6 eV) was employed as an X-ray source. Emitted electrons were detected at angles between 23° and 83°. Spectra were calibrated based on the Au $4f_{7/2}$ peak of 87.6 eV. TDS measurements were carried out using a WA-1000S (ESCO Ltd., Japan) in an ultrahigh vacuum chamber (3×10^{-7} Pa) with a quadrupole mass spectrometer (OMG-422, Balzers). The heating rate was 1 K/s. Surface temperature was monitored by a thermocouple in tight contact with the sample. Pressure in the chamber was increased up to $\sim 10^{-6}$ Pa during measurements.

RESULTS AND DISCUSSION

Surface Structure of MS Monolayers as a Function of Deposition Time. To understand self-assembly behaviors of MSe on Au(111), it is helpful to first examine and compare MS monolayers under identical conditions. In general, short-chain alkanethiolate SAMs are known to lack significant van der Waals interactions. Thus, they usually exhibit poor packing density compared with longer-chain thiolate SAMs given the same deposition time.[52,53] Furthermore, adsorption rates of dialkyl disulfides on gold surfaces are typically lower than those of alkanethiols having the identical chain structure.[54] SAM formations of dialkyl diselenides are sensitive to the solution concentrations; especially diselenides with short-chains hardly form well-ordered SAMs from solution-phase deposition.[35,51]

To overcome the difficulties noted above, we adopted a vapor-phase deposition method at an elevated temperature of 323 K to rule out solvent-mediated effects and promote SAM formation. Figure 1 shows the structural changes in MS

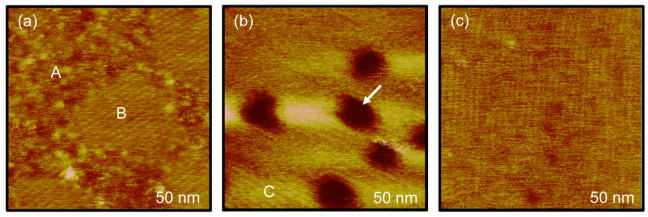

Figure 1. STM images of MS monolayers on Au(111) prepared from DMDS by vapor deposition at 323 K for (a) 1 h, (b) 2 h, and (c) 24 h. All scan sizes were 50 nm × 50 nm.

monolayers prepared using the vapor deposition method as a function of deposition time (see also large-scale STM images in Figure S1 of the Supporting Information). After a 1 h deposition, both a disordered phase (indicated by A) and long-range ordered row phase (indicated by B) were observed (Figure 1a), which are typical of organosulfur SAMs formed with a low packing density. It was previously reported that methanethiol monolayers can also form cognate long-range row phases of $(2\sqrt{3} \times \sqrt{3})R30°$ and $(3 \times 2\sqrt{3})$ structures.[53] On the basis of our estimates, the row phase with lateral dimension of several nanometers had a corrugation period of $\sim 1.51 \pm 0.06$

dx.doi.org/10.1021/jp409531w | J. Phys. Chem. C 2014, 118, 8322−8330

nm, slightly larger than 1.25 nm and shorter than 2.1 nm, which were the periods observed for MS monolayers prepared from 1 and 50 mM ethanol solutions at room temperature after 1 h deposition, respectively.[55] This study suggested that MS monolayer formations exhibit abnormal assembly behaviors that are dependent on the solution concentration.[55] These unusual adsorption behaviors (changes in packing structure and adsorption condition depending on solution concentration) in the formation of MS monolayers from DMDS molecules on Au(111) were often observed when they were prepared from solution-phase depositions.[55,56] Meanwhile, because the vapor deposition method does not involve such unusual adsorption behaviors, it gave rise to consistent corrugation periods independent of deposition time up to 2 h.

In general, the appearance of vacancy islands (VIs) in alkanethiolate SAMs strongly suggest that SAM formation has occurred via a chemical interaction between the gold surface and adsorbed molecules,[6,8,26,27] providing evidence for formation of MS monolayers via cleavage of S−S bonds, as in the case of dialkyl disulfides with longer alkyl chains.[7,56−59] As deposition time increased to 2 h, the disordered phases disappeared and VIs (indicated by the white arrow) emerged as shown in Figure 1b and Figure S1b (Supporting Information). The corrugation period of the row phase (indicated by C) changed from 1.51 ± 0.06 to 1.23 ± 0.03 nm. This structural transition may have been driven by an increase in intermolecular and molecule−substrate interactions.

Although the growth kinetics of SAMs by dialkyl disulfides are slower than for alkanethiols with an identical alkyl chain length,[54,55] dialkyl disulfides are known to form alkanethiolate SAMs as a result of S−S bond cleavage. Hayashi et al. suggested that DMDS also prefers S−S bond cleavage during MS monolayer formation.[57] In general, long-chain alkanethiolate SAMs exhibit higher packing density as deposition time increases.

Meanwhile, upon increasing the deposition time to 24 h, we found that the density of VIs decreased in comparison to MS monolayers formed after a 2 h deposition (Figure 1c). Likewise, the STM image became faint, which may be due to changes in adsorption condition and structure of the monolayers resulting from the insertion of a trace amount of DMDS molecules for longer deposition. This result is consistent with XPS results showing a small increase of unbound sulfur peak (the details will be discussed later in Figure 4a and Table 1). The similar faint STM image was also observed for MS monolayers containing the unbound DMDS molecules prepared from a high concentrated solution (50 mM) of DMDS.[55] The decrease in the density of VIs was attributed to the ostwald ripening process, which can be accelerated by thermal annealing or, in the case of SAMs, very weak intermolecular interactions.[53,60] Cometto et al. proposed that longer deposition using an ethanol solution results in oxidation of MS monolayers, leading to its decomposition to atomic sulfur and formaldehyde via S−C cleavage.[56]

The vapor deposition method employed in this study may not have been involved in oxidation processes. Specifically, the observation of faint images may have been due to gradual adsorption or insertion of incoming DMDS molecules into monolayers during long depositions, resulting in decreased ordering of MS monolayers. Such adsorption behavior can occur easily when intermolecular interactions are very weak, because the methyl molecular backbones in the monolayers on Au(111) cannot effectively block the adsorption or insertion of incoming molecules. This possibility was supported by our XPS results shown below (Figure 4a and Table 1). Lastly, similar structural behavior was observed when MS monolayers were formed in a highly concentrated solution of 50 mM.[51]

Table 1. XPS Peak Ratio of S 2p/Au 4f for MS Monolayers Prepared from DMDS by Vapor Deposition at 323 K for 1, 2, and 24 h

sample	S 2p species	peak (eV)	S 2p/Au 4f[a]	S2[b]/S1[c]
DMDS, 1 h	S1 2p	160.80	0.000903	13.37
		162.00		
	S2 2p	162.09	0.012074	
		163.29		
	S1 2p + S2 2p	–	0.012977	
DMDS, 2 h	S1 2p	161.06	0.002368	4.75
		162.26		
	S2 2p	162.04	0.011254	
		163.24		
	S3 2p	163.6	0.001325	
		164.8		
	S1 2p + S2 2p + S3 2p	–	0.014947	
DMDS, 24 h	S1 2p	161.06	0.003059	3.44
		162.26		
	S2 2p	162.02	0.010538	
		163.22		
	S3 2p	163.41	0.001903	
		164.61		
	S1 2p + S2 2p + S3 2p	–	0.015500	

[a]Au $4f_{7/2}$. [b]S2 2p. [c]S1 2p.

Surface Structure of MSe Monolayers as a Function of Deposition Time. The formation and structure of MSe monolayers were monitored as a function of deposition time using identical experimental conditions for MS monolayers (Figure 2 and Figure S2 (large-scale STM images in the Supporting Information)). After a 1 h deposition, MSe monolayers also exhibited a long-ranged-ordered row phase via cleavage of Se−Se from DMDSe. Interestingly, we observed round or triangular shape VIs for alkanethiolate SAMs on Au(111), whereas MSe monolayers contained VIs with a straight-edge structure (indicated by the white arrow), as shown in Figure 2a. This result may have been an intrinsic structural characteristic for MSe monolayers resulting from a difference in binding volume due to the difference in van der Waals radius of sulfur (1.85 Å) and selenium (2.0 Å) against the Au(111) surface.[43] In addition, slightly higher interaction strength of selenium headgroups than that of sulfurs toward the Au(111) surface may be responsible for the difference. Interestingly, these VIs existed in the direction parallel to the

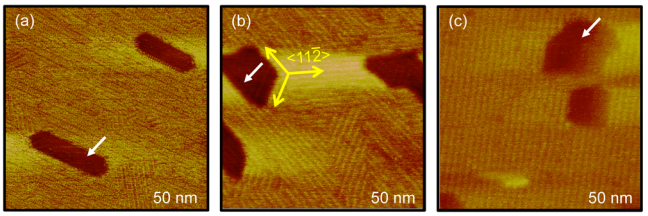

Figure 2. STM images of MSe monolayers on Au(111) prepared from DMDSe by vapor deposition at 323 K for (a) 1 h, (b) 2 h, and (c) 24 h. All scan sizes were 50 nm × 50 nm.

dx.doi.org/10.1021/jp409531w | J. Phys. Chem. C 2014, 118, 8322−8330

row phases with three domain orientations (indicated by yellow arrows for substrate $\langle 11\bar{2}\rangle$ direction), suggesting that the VIs are formed due to the 3-fold symmetry of Au(111) surface.[34]

The corrugation period of the row phase was 6.3 ± 0.4 Å; however, as the deposition time increased to 2 h, the corrugation period of bright molecular rows increased to 13.0 ± 0.7 Å, which is exactly twice the period of the case of 1 h deposition (Figure 2b). Additional structural details for MSe monolayers are discussed below (Figure 3). Although we did

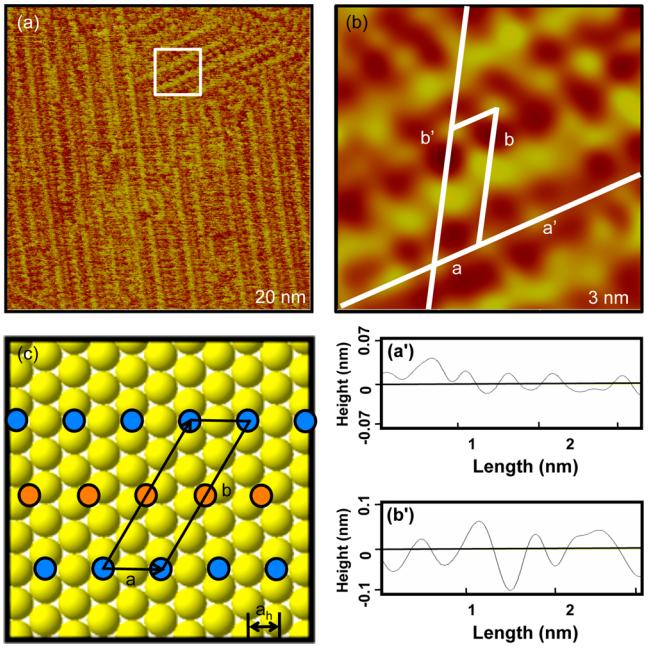

Figure 3. (a) Molecularly resolved STM image (20 nm × 20 nm) of MSe monolayers on Au(111) prepared by vapor deposition at 323 K for 1 h. (b) 2D filtered STM image of a rectangular region in Figure 3a showing the row structure of MSe monolayers. (a′) and (b′) are line profiles along lines a′ and b′ on the image, which show the high periodicities of the adsorbed molecules. (c) A proposed structural model of MSe monolayers with a row phase, which was described as a $(\sqrt{3} \times 3\sqrt{3})R30°$ structure.

not observe any individual molecular structure, our STM measurements provided clear evidence of monolayer structure formed with long-range-ordered row phases (Figure 2b). Recent STM and contact angle studies revealed that OSe SAMs prepared from solution deposition undergo a phase transition from an ordered structure to a disordered structure at an initial stage after deposition for 5 min.[34] On the basis of these results, the authors proposed that the stronger binding affinity of selenium headgroups toward gold surfaces compared with sulfur may be responsible for their atypical adsorption behaviors. In addition, their solvent-mediated etching of SAMs via oxidation of selenium headgroups may also result in the abnormal adsorptions.[34] In the present study, we did not observe any apparent evidence on the phase transition with MSe monolayers after a 2 h deposition using the vapor deposition method. It should also be noted that the size and density of VIs were not significantly influenced as deposition time increased to 2 h (see Figure S2, Supporting Information).

After 24 h deposition, we noticed that the surface structure of MSe monolayers with the long-ranged row phases was faintly visualized compared to that of MSe monolayers formed after deposition for 2 h (Figure 2c and Figure S2c, Supporting Information). These results showed good similarity with MS monolayers formed after 24 h deposition (Figure 1c). On the basis of the XPS results (Figure 4b and Table 2), we suggest

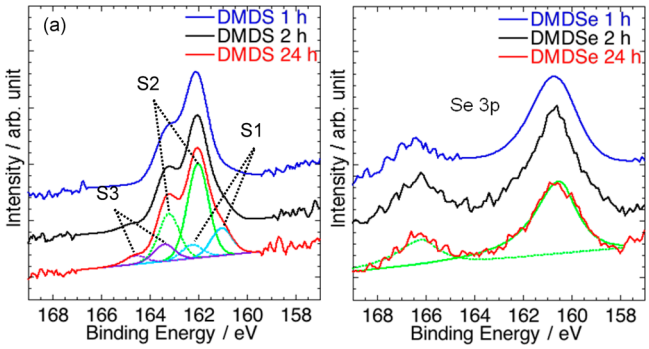

Figure 4. XPS spectra in (a) the S 2p region of MS and (b) the Se 3p region of MSe monolayers on Au(111) prepared from DMDS and DMDSe by vapor deposition at 323 K, respectively. MS monolayers were composed of three different sulfur species: S1, S2, and S3 sulfur peaks each split into a doublet. The solid curves correspond to the S $2p_{3/2}$ peak, and the dotted curves correspond to the S $2p_{1/2}$ peak.

that the desorption of some DMDSe molecules adsorbed on Au(111) may lead to a decrease in crystalline monolayer structures, resulting in faint imaging contrast.

Table 2. XPS Peak Ratio of Se 3p/Au 4f for MSe Monolayers Prepared from DMDSe by Vapor Deposition at 323 K for 1, 2, and 24 h

sample	Se 3p species	peak (eV)	Se 3p/Au 4f
DMDSe, 1 h	Se 3p	160.66	0.010304
		166.30	
DMDSe, 2 h	Se 3p	160.64	0.012194
		166.20	
DMDSe, 24 h	Se 3p	160.53	0.009474
		166.19	

Figure 3a shows an ordered molecular row structure of MSe monolayers on Au(111) formed after deposition for 1 h at 323 K. To resolve the molecular structure, we investigated the rectangular area in Figure 3a. Looking carefully at the row phases, we observed dark molecular rows between two neighboring bright molecular rows. On the basis of our STM measurement, we extracted the lattice constant of an oblique rectangular unit cell composed of two molecules as shown in Figure 3b: a = 5.0 Å = $\sqrt{3}a_h$ and b = 14.9 Å = $3\sqrt{3}a_h$, where a_h = 2.89 Å corresponds to the interatomic distance of the Au(111) lattice. The line profiles along lines a′ and b′ indicated in Figure 3b show the periodicities of the adsorbed molecules. A schematic structural model of MSe monolayers on Au(111) is shown in Figure 3c. The molecular packing structure of monolayers consisted of a $(\sqrt{3} \times 3\sqrt{3})R30°$ superlattice containing two molecules for each oblique rectangular unit cell, which is comparable to the packing structures for MS monolayers containing two different row phases of $(2\sqrt{3} \times \sqrt{3})R30°$ and $(3 \times 2\sqrt{3})$ structures.[53] The average area molecular density for MSe monolayers on Au(111) was calculated as 37.5 Å^2/molecule. The structural model in Figure 3c strongly suggested that selenolate SAMs had a row structure that usually appears prior to the formation of closely packed SAMs. An analogous row phase of $(\sqrt{3} \times 3\sqrt{3})R30°$ has been

dx.doi.org/10.1021/jp409531w | J. Phys. Chem. C 2014, 118, 8322−8330

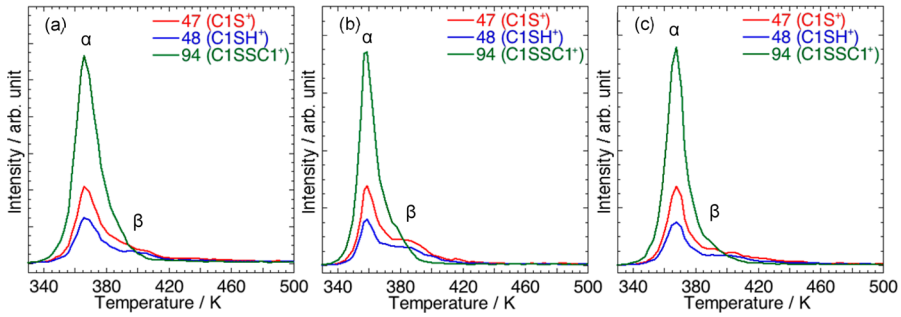

Figure 5. TDS spectra of MS monolayers on Au(111) prepared from DMDS by vapor deposition at 323 K for (a) 1 h, (b) 2 h, and (c) 24 h.

observed for dodecaneselenolate SAMs with a longer alkyl chain.[61] Meanwhile, the recent theoretical work using density functional theory reported that the bridge site for MSe on Au(111) is the most stable adsorption site compared to other sites.[36] Thus, we adopt the bridge site adsorption model for describing the surface structure of MSe monolayers on Au(111) (Figure 3c).

Adsorption Behaviors of MS and MSe Monolayers on Au(111). To elucidate binding states of both SAMs, we next examined XPS spectra of MS and MSe monolayers prepared from DMDS and DMDSe by vapor-phase deposition at 323 K, respectively. Figure 4a shows the S 2p XPS spectra of MS monolayers as a function of deposition time. In general, doublet peaks stemmed from S $2p_{3/2}$ and S $2p_{1/2}$ splitting with an intensity ratio of 2:1 are observed for alkanethiolate SAMs.[13,26,27,62,63] The solid and dotted lines of the fitted curves in Figure 4a corresponded to S $2p_{3/2}$ and S $2p_{1/2}$ peaks, respectively. Strong S1 peaks usually appear at around 161 and 162.2 eV for thiolate SAMs with a low coverage or disordered phase, whereas for thiolate SAMs with a well-ordered phase, the appearance of strong S2 peaks at 162.0 and 163.2 eV became dominant.[13,26,27,62−64] Both the S1 and S2 peaks were ascribed to bound sulfur species. Meanwhile, S3 peaks are primarily observed at around 163.5 and 164.7 eV for SAMs with unbound sulfurs or physisorbed multilayers.[13,65] Regardless of deposition time, all samples exhibited strong S2 peaks rather than S1 peaks. As the immersion time increased to 2 h, S3 peaks surprisingly emerged, which gradually increased during deposition for 24 h. Table 1 summarizes the sulfur peak positions and relative intensity ratios for S 2p/Au 4f and S2/S1 peaks of MS monolayers on Au(111) prepared from vapor deposition at 323 K. In contrast with the STM results, the XPS results indicated that a 1 h deposition was associated with a higher S2/S1 ratio than 2 h deposition, resulting in a slowly decreasing S2/S1 ratio as the deposition time increased to 24 h. This decrease was attributed to a remarkable increase in the intensity of the S1 peak, especially after deposition for 2 h, and a gradual decrease in the intensity of the S2 peak from 2 h until 24 h. Consequently, the total coverage of bound sulfurs was almost quantitatively identical for all cases of different deposition times. Moreover, the unbound S3 sulfurs, which began to appear after deposition for 2 h, then increased up to deposition for 24 h. These results were consistent with our STM results. As such, we inferred that the increase in the intensity of the S1 and S3 species was responsible for the observation of faint STM imaging from monolayer samples prepared after longer deposition.

We next examined Se 3p XPS spectra for MSe monolayers, whose results are shown in Figure 4b. Fitting of all three spectra exhibited doublet Se $3p_{3/2}$ and Se $3p_{1/2}$ peaks at 160.7 and 166.2 eV, respectively, which was in good agreement with previous reports of organoselenolate SAMs on metal surfaces.[50,66,67] We summarized the selenium peak positions and the relative intensity ratios for Se 3p/Au 4f as shown in Table 2. We observed that the surface coverage of Se 3p species increased by 18% until 2 h deposition and then the surface coverage decreased by 22% after 24 h deposition compared with the 2 h deposition. Presently, we do not understand why the surface coverage of MSe monolayers decreased with increasing deposition time for 24 h at 323 K. One possible explanation is that, after the formation of closely packed MSe monolayers on Au(111), partial desorption of selenolate molecules may have occurred slowly at a high temperature during the longer deposition time, which may be more favorable than adsorption of DMDSe molecules. Therefore, the crystalline structure of MSe monolayers should have decreased, as suggested by our STM results. On the other hand, we excluded oxidation of selenolate as a cause of the decrease in surface coverage because we could not observe a peak for SeO_2 at around 59.8 eV.[45]

Thermal Desorption Behaviors of MS and MSe Monolayers on Au(111). To understand the effect of headgroups on the thermal desorption behaviors of MS and MSe monolayers on Au(111), we examined and compared both monolayers prepared after vapor-phase deposition at 323 K as a function of deposition time. Figure 5 shows the TDS spectra of MS monolayers prepared after deposition of DMDS for (a) 1 h, (b) 2 h, and (c) 24 h. We monitored three main desorption fragments for methanethiolate (C_1S^+, monomer, m/z = 47), methanethiol (C_1SH^+, thiol, m/z = 48), and DMDS ($C_1SSC_1^+$, dimer, m/z = 94) on Au(111) surfaces, as shown in Figure 5. The three desorption fragments with a sharp and strong intensity (indicated by an α peak) were observed at around 366 K, while shoulder peaks with a broad, weak intensities (indicated by a β peak) for the same fragments were also observed with a slightly higher surface temperature region. We also observed that desorption for dimers, thiolates, and thiols were initiated at approximately 335, 350, and 355 K, respectively. In general, desorption of dimers usually occurs at a lower temperature compared with thiolates and thiols. It is well known that dimerization of two neighboring sulfur atoms in alkanethiolate SAMs on gold surfaces occurs readily during thermal heating, resulting in desorption of dimer fragments under ultrahigh vacuum conditions.[68−73] The desorption intensity for dimers from MS monolayers derived from the adsorption of DMDS molecules on Au(111) was much stronger than for monomers or thiols (Figure 5), implying that desorption of dimers was more energetically favorable than

dx.doi.org/10.1021/jp409531w | J. Phys. Chem. C 2014, 118, 8322−8330

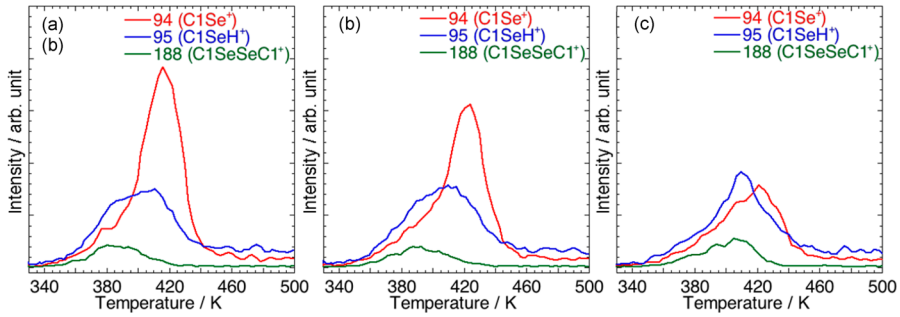

Figure 6. TDS spectra of MSe monolayers on Au(111) prepared from DMDSe by vapor deposition at 323 K for (a) 1 h, (b) 2 h, and (c) 24 h.

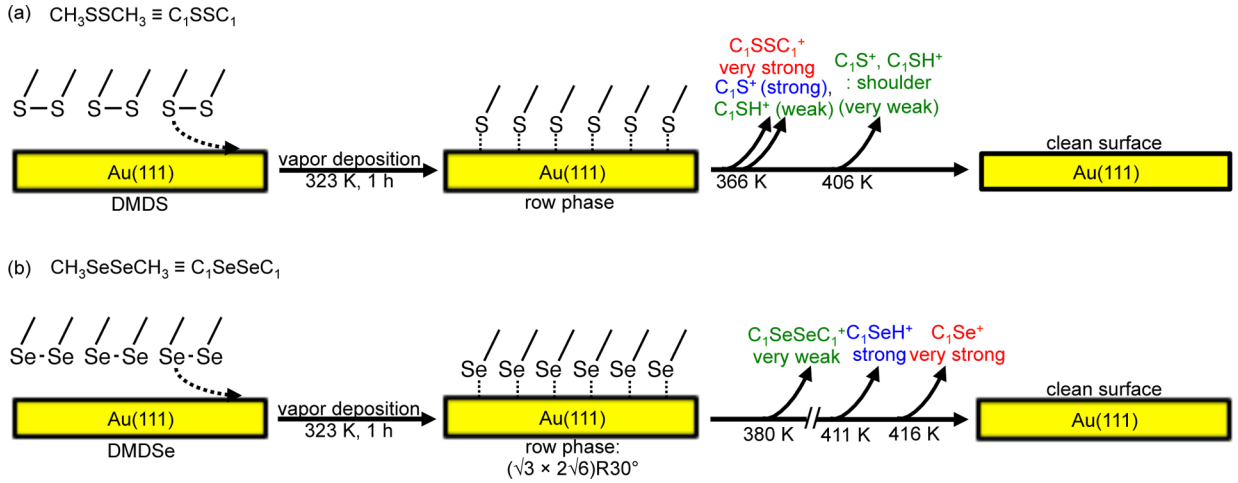

Figure 7. Schematic view describing different thermal desorption behaviors of (a) MS monolayers and (b) MSe monolayers on Au(111) prepared from DMDS and DMDSe by vapor deposition at 323 K for 1 h, respectively.

those of monomers or thiols.[69,71] Similar desorption behavior for dimers have also been observed for SAMs prepared by octanethiol with a longer alkyl chain.[61] Recently, it was reported that dimerization is strongly influenced by surface morphology of substrates. Specifically, dimerization was shown to occur more efficiently on the Au(111) surface containing atomically flat terraces compared with polycrystalline gold substrates containing abundant nanosized grains. Moreover, dimerization can take place more effectively in a closely packed standing-up phase rather than in a low coverage lying-down stripe phase.[69,70] On the other hand, a previous study on undecanethiol SAMs indicated that the α peak originates from desorption of chemisorbed molecules from a closely packed phase, while the β peak originates from desorption of chemisorbed molecules in a loosely packed phase formed after strong desorption of molecules at lower temperature regions.[62]

Desorption peaks with a strong intensity for methanethiolates (C_1S^+) and methanethiols (C_1SH^+) on Au(111) were observed at the same temperature of 366 K, which was identical for dimers. Desorption of methanethiolates occurs mainly via S–Au bond cleavage in thiolate SAMs on the Au(111) surface, as well as from doubly ionized disulfide fragments as reported for alkanethiol SAMs with longer alkyl chains.[61−65] Previous studies have suggested that the desorption peak of thiols originate from a hydrogen abstract reaction of thiolates from the inside of a chamber and/or surface hydrogenation of thiolates.[61−64] We found that the thermal desorption behaviors of MS monolayers prepared using solution-phase deposition were different from our results obtained with vapor-phase deposition. Specifically, the intensity of the dimer was weaker than those of thiolates and thiols, the peaks of which were observed at a slightly higher surface temperature.[64] These results suggest that the thermal desorption behaviors of MS monolayers were significantly influenced by preparation conditions. On the other hand, the relative desorption intensities of monomer to thiol fragments were calculated as 1.68, 1.71, and 1.80 for deposition times of 1 h, 2 h, and 24 h, respectively. Likewise, the relative desorption intensities of dimer to methanethiol fragments were calculated as 4.57, 4.61, and 5.01 for deposition times of 1 h, 2 h, and 24 h, respectively. Although the relative desorption intensities of monomers or dimers to thiol gradually increased as a function of deposition time, the associated variations in intensity were minimal. This observation was attributed to the nearly identical surface coverage of methanethiolates chemisorbed on Au(111) surfaces regardless of deposition time, suggesting that all samples reached to the fully covered phase, which was further supported by XPS and TDS results.

To investigate the effect of headgroups on thermal desorption behaviors, we monitored three main desorption fragments for methaneselenolate (C_1Se^+, monomer, m/z = 94), methaneselenol (C_1SeH^+, selenol, m/z = 95), and DMDSe ($C_1SeSeC_1^+$, dimer, m/z = 188) from DMDSe assemblies on Au(111) obtained using identical preparation conditions for MS monolayers (Figure 6).

Interestingly, we found that thermal desorption behaviors of MSe monolayers were markedly different from those of MS monolayers, as shown in Figures 5 and 6. Three remarkable differences between thiolate and selenolate SAMs were

dx.doi.org/10.1021/jp409531w | J. Phys. Chem. C 2014, 118, 8322−8330

observed. First, all three thermal desorption peaks for MSe monolayers were observed at higher temperatures compared with those of MS monolayers. Second, we noted that monomer peaks were more prominent than dimer peaks as summarized in Figure 7. This result implied that dimerization of MSe molecules was significantly suppressed during thermal desorption process. The higher desorption temperature and the lower efficient dimerization for MSe monolayers on Au(111) strongly suggested that the interactions between headgroups and gold surfaces for MSe monolayers are stronger than for MS monolayers.[34−37,39,42−47] Thus, the stronger affinity of selenium headgroups toward gold surfaces may prevent dimerization of neighboring MSe molecules. It was recently demonstrated that as the bond strength between sulfur and metal increases, dimerization of sulfur headgroups is largely suppressed.[69] Therefore, our TDS results provide strong evidence that the binding affinity of selenium against gold was much stronger than that of sulfur because our system is mainly involved in headgroup−-surface interactions. Third, we observed that desorption peaks for methanethiol and methanethiolate fragments were observed at nearly the same temperature of 366 K. Moreover, alkanethiols SAMs with the longer alkyl chains showed that desorption of alkanethiolate fragments usually occurred prior to that of alkanethiol fragments at a lower temperature.[68−70] Different from alkanethiol SAMs, desorption of methaneselenol fragments arose prior to desorption of methaneselenolates. Specifically, methaneselenolates thermally desorb at 416−424 K, while the desorption peaks of methaneselenols appeared at 410−411 K, as shown in Figure 6. This observation suggested that methaneselenolates reacted effectively with surrounding hydrogen atoms to form methaneselenol desorption fragments before their desorption, resulting in the desorption of selenol fragments at a lower temperature. Meanwhile, as the deposition time increased, the relative desorption intensities of monomers to methaneselenols decreased in the order of 2.54, 1.98, and 0.86, while those of dimers were almost identical quantitatively, in the order of 0.28, 0.25, and 0.30, respectively.

At present, it is difficult to understand the unusual thermal desorption behavior of methaneselenolates. A possible explanation may be the delicate change in adsorption condition and geometry of selenolates on Au(111) after a long deposition time, which could not be detected by XPS. In contrast to alkanethiols SAMs, we recently observed that ordered alkaneselenolate SAMs can only be obtained by using a micromolar solution and very short immersion time (less than 30 min), suggesting that surface characteristics for selenolate SAMs can be modified by deposition time.[34,35]

CONCLUSIONS

In this study, self-assemblies of DMDS and DMDSe molecules on Au(111) were investigated using STM, XPS, and TDS to understand the effect of headgroups (i.e., sulfur and selenium) on the formation of their respective monolayers, thermal stability, and thermal desorption behaviors. To alleviate solvent-mediated effects, we employed ambient vapor deposition method at an elevated temperature, 323 K. XPS measurements showed that MS or MSe monolayers chemisorbed on Au(111) formed via S−S bond cleavage of DMDS or Se−Se bond cleavage of DMDSe, respectively. STM observations showed that adsorption of DMDS molecules on Au(111) after deposition for 1 h generated MS monolayers containing a disordered phase and ordered row phase with an inter-row spacing of 1.51 nm. On the other hand, the adsorption of DMDSe molecules led to the formation of long-range-ordered MSe monolayers containing VIs with a unique straight-edge structure. The packing structure for the MSe monolayer was determined to be a $(\sqrt{3} \times 3\sqrt{3})R30°$ superlattice, which was different from that of the MS monolayer, which has $(2\sqrt{3} \times \sqrt{3})R30°$ and $(3 \times 2\sqrt{3})$ structures. XPS measurements revealed that the adsorption of DMDS and DMDSe molecules on Au(111) generated MS and MSe monolayers chemisorbed on Au(111) via S−S bond cleavage of DMDS or Se−Se bond cleavage of DMDSe, respectively. Using TDS, we monitored three main desorption fragments for MS and MSe monolayers: a monomer (CH_3S^+, CH_3Se^+), a parent mass species monomer (CH_3SH^+, CH_3SeH^+), and a dimer monomer ($CH_3S{-}SCH_3^+$, $CH_3Se{-}SeCH_3^+$). The TDS results demonstrated that thermal desorption behaviors of MSe monolayers were markedly different from those of MS monolayers. All desorption peaks for MSe monolayers appeared at a higher temperature compared with MS monolayers, suggesting that the adsorption affinity of selenium atoms in SAMs on Au(111) surfaces is stronger than that of sulfur atoms. We also found that the desorption intensity of dimer fragments for MSe monolayers was much lower than that of MS monolayers, indicating that dimerization of selenolate SAMs on Au(111) could not occur efficiently during thermal heating compared with thiolate SAMs. These results provide meaningful information for understanding the headgroup effect on the formation, structure, thermal stability, and desorption behavior of monolayers on Au(111) prepared from DMDS and DMDSe molecules containing methyl groups.

ASSOCIATED CONTENT

Supporting Information

Additional STM images of MS and MSe monolayers. This material is available free of charge via the Internet at http://pubs.acs.org.

AUTHOR INFORMATION

Corresponding Authors

*(S.Y.L.) Phone: +82-2-2220-0908; fax: +82-2-2296-0287; e-mail: yunnylee@hanyang.ac.kr.

*(J.N.) Phone: +82-2-2220-0938; fax: +82-2-2299-0762; e-mail: jgnoh@hanyang.ac.kr.

Notes

The authors declare no competing financial interest.

ACKNOWLEDGMENTS

This research was supported by Basic Science Research Program through the National Research Foundation of Korea (NRF) funded by the Ministry of Education (NRF-2013-R1A1A2009781 and NRF-2012R1A6A1029029). S.Y.L. thanks Prof. Justyn Jaworski (Hanyang University, Seoul, Korea) for the helpful comments.

REFERENCES

(1) Lee, W.; Kim, E. R.; Lee, H. Chemical Approach to High-Resolution Patterning on Self-Assembled Monolayers Using Atomic Force Microscope Lithography. *Langmuir* **2002**, *18*, 8375−8380.

(2) Park, J.; Lee, H. Effect of Surface Functional Groups on Nanostructure Fabrication Using AFM Lithography. *Mater. Sci. Eng., C* **2004**, *24*, 311−314.

(3) Nakamura, F.; Ito, E.; Hayashi, T.; Hara, M. Fabrication of COOH-Terminated Self-Assembled Monolayers for DNA Sensors. *Colloids Surf., A* **2006**, *284*, 495−498.
(4) Hamoudi, H.; Guo, Z. A.; Prato, M.; Dablemont, C.; Zheng, W. Q.; Bourguignon, B.; Canepa, M.; Esaulov, V. A. On the Self Assembly of Short Chain Alkanedithiols. *Phys. Chem. Chem. Phys.* **2008**, *10*, 6836−6841.
(5) Love, J. C.; Estroff, L. A.; Kriebel, J. K.; Nuzzo, R. G.; Whitesides, G. M. Self-Assembled Monolayers of Thiolates on Metals as a Form of Nanotechnology. *Chem. Rev.* **2005**, *105*, 1103−1169.
(6) Noh, J.; Hara, M. Final Phase of Alkanethiol Self-Assembled Monolayers on Au(111). *Langmuir* **2002**, *18*, 1953−1956.
(7) Noh, J.; Kato, H. S.; Kawai, M.; Hara, M. Surface and Adsorption Structures of Dialkyl Sulfide Self-Assembled Monolayers on Au(111). *J. Phys. Chem. B* **2002**, *106*, 13268−13272.
(8) Ulman, A. Formation and Structure of Self-Assembled Monolayers. *Chem. Rev.* **1996**, *96*, 1533−1554.
(9) Liu, G. Y.; Xu, S.; Qian, Y. L. Nanofabrication of Self-Assembled Monolayers Using Scanning Probe Lithography. *Acc. Chem. Res.* **2000**, *33*, 457−466.
(10) Gorman, C. B.; He, Y. F.; Carroll, R. L. The Influence of Headgroup on the Structure of Self-Assembled Monolayers as Viewed by Scanning Tunneling Microscopy. *Langmuir* **2001**, *17*, 5324−5328.
(11) Ito, E.; Konno, K.; Noh, J.; Kanai, K.; Ouchi, Y.; Seki, K.; Hara, M. Chain Length Dependence of Adsorption Structure of COOH-Terminated Alkanethiol Sams on Au(111). *Appl. Surf. Sci.* **2005**, *244*, 584−587.
(12) Konno, K.; Ito, E.; Noh, J.; Hara, M. Surface Structures and Adsorption States of Self-Assembled Monolayers Formed by Various COOH-Terminated Alkanethiols on Au(111). *Jpn. J. Appl. Phys.* **2006**, *45*, 405−408.
(13) Lee, S. Y.; Noh, J.; Ito, E.; Lee, H.; Hara, M. Solvent Effect on Formation of Cysteamine Self-Assembled Monolayers on Au(111). *Jpn. J. Appl. Phys.* **2003**, *42*, 236−241.
(14) Shuang, L.; Cao, P.; Colorado, R.; Yan, X. P.; Wenzl, I.; Shmakova, O. E.; Graupe, M.; Lee, T. R.; Perry, S. S. Local Packing Environment Strongly Influences the Frictional Properties of Mixed CH_3- and CF_3-Terminated Alkanethiol Sams on Au(111). *Langmuir* **2005**, *21*, 933−936.
(15) Tamada, K.; Nagasawa, J.; Nakanishi, F.; Abe, K.; Hara, M.; Knoll, W.; Ishida, T.; Fukushima, H.; Miyashita, S.; Usui, T.; Koini, T.; Lee, T. R. Structure of SAMs Generated from Functionalized Thiols on Gold. *Thin Solid Films* **1998**, *327*, 150−155.
(16) Tsukamoto, K.; Kubo, T.; Nozoye, H. Structure of Mercaptoalcohol Self-Assembled Monolayers on Au(111). *Appl. Surf. Sci.* **2005**, *244*, 578−583.
(17) Wang, H.; Chen, S. F.; Li, L. Y.; Jiang, S. Y. Improved Method for the Preparation of Carboxylic Acid and Amine Terminated Self-Assembled Monolayers of Alkanethiolates. *Langmuir* **2005**, *21*, 2633−2636.
(18) Poirier, G. E. Characterization of Organosulfur Molecular Monolayers on Au(111) Using Scanning Tunneling Microscopy. *Chem. Rev.* **1997**, *97*, 1117−1127.
(19) Azzam, W.; Bashir, A.; Shekhah, O. Thermal Study and Structural Characterization of Self-Assembled Monolayers Generated from Diadamantane Disulfide on Au(1 1 1). *Appl. Surf. Sci.* **2011**, *257*, 3739−3747.
(20) Jia, J. J.; Mukherjee, S.; Hamoudi, H.; Nannarone, S.; Pasquali, L.; Esaulov, V. A. Lying-Down to Standing-Up Transitions in Self Assembly of Butanedithiol Mono Layers on Gold and Substitutional Assembly by Octanethiols. *J. Phys. Chem. C* **2013**, *117*, 4625−4631.
(21) Cai, L. T.; Yao, Y. X.; Yang, J. P.; Price, D. W.; Tour, J. M. Chemical and Potential-Assisted Assembly of Thiolacetyl-Terminated Oligo(Phenylene Ethynylene)S on Gold Surfaces. *Chem. Mater.* **2002**, *14*, 2905−2909.
(22) Lukkari, J.; Meretoja, M.; Kartio, I.; Laajalehto, K.; Rajamaki, M.; Lindstrom, M.; Kankare, J. Organic Thiosulfates (Bunte Salts): Novel Surface-Active Sulfur Compounds for the Preparation of Self-Assembled Monolayers on Gold. *Langmuir* **1999**, *15*, 3529−3537.
(23) Tour, J. M.; Jones, L.; Pearson, D. L.; Lamba, J. J. S.; Burgin, T. P.; Whitesides, G. M.; Allara, D. L.; Parikh, A. N.; Atre, S. V. Self-Assembled Monolayers and Multilayers of Conjugated Thiols, α,ω-Dithiols, and Thioacetyl-Containing Adsorbates. Understanding Attachments between Potential Molecular Wires and Gold Surfaces. *J. Am. Chem. Soc.* **1995**, *117*, 9529−9534.
(24) Lusk, A. T.; Jennings, G. K. Characterization of Self-Assembled Monolayers Formed from Sodium S-Alkyl Thiosulfates on Copper. *Langmuir* **2001**, *17*, 7830−7836.
(25) Lau, K. H. A.; Huang, C.; Yakovlev, N.; Chen, Z. K.; O'Shea, S. J. Direct Adsorption and Monolayer Self-Assembly of Acetyl-Protected Dithiols. *Langmuir* **2006**, *22*, 2968−2971.
(26) Lee, S. Y.; Choi, Y.; Ito, E.; Hara, M.; Lee, H.; Noh, J. Growth, Solvent Effects, and Thermal Desorption Behavior of Octylthiocyanate Self-Assembled Monolayers on Au(111). *Phys. Chem. Chem. Phys.* **2013**, *15*, 3609−3617.
(27) Choi, Y.; Jeong, Y.; Chung, H.; Ito, E.; Hara, M.; Noh, J. Formation of Ordered Self-Assembled Monolayers by Adsorption of Octylthiocyanates on Au(111). *Langmuir* **2008**, *24*, 91−96.
(28) Ciszek, J. W.; Stewart, M. P.; Tour, J. M. Spontaneous Assembly of Organic Thiocyanates on Gold Sufaces. Alternative Precursors for Gold Thiolate Assemblies. *J. Am. Chem. Soc.* **2004**, *126*, 13172−13173.
(29) Ciszek, J. W.; Tour, J. M. Mechanistic Implications of the Assembly of Organic Thiocyanates on Precious Metals. *Chem. Mater.* **2005**, *17*, 5684−5690.
(30) Dreesen, L.; Volcke, C.; Sartenaer, Y.; Peremans, A.; Thiry, P. A.; Humbert, C.; Grugier, J.; Marchand-Brynaert, J. Comparative Study of Decyl Thiocyanate and Decanethiol Self-Assembled Monolayers on Gold Substrates. *Surf. Sci.* **2006**, *600*, 4052−4057.
(31) Shen, C.; Buck, M.; Wilton-Ely, J. D. E. T.; Weidner, T.; Zharnikov, M. On the Importance of Purity for the Formation of Self-Assembled Monolayers from Thiocyanates. *Langmuir* **2008**, *24*, 6609−6615.
(32) *CRC Handbook of Chemistry and Physics*, 92nd ed.; CRC Press: Boca Raton, FL, 2012.
(33) Bandyopadhyay, K.; Vijayamohanan, K.; Venkataramanan, M.; Pradeep, T. Self-Assembled Monolayers of Small Aromatic Disulfide and Diselenide Molecules on Polycrystalline Gold Films: A Comparative Study of the Geometrical Constraint Using Temperature-Dependent Surface-Enhanced Raman Spectroscopy, X-Ray Photoelectron Spectroscopy, and Electrochemistry. *Langmuir* **1999**, *15*, 5314−5322.
(34) Choi, J.; Kang, H.; Ito, E.; Hara, M.; Noh, J. Phase Transition of Octaneselenolate Self-Assembled Monolayers on Au(111) Studied by Scanning Tunneling Microscopy. *Bull. Korean Chem. Soc.* **2011**, *32*, 2623−2627.
(35) Choi, J.; Lee, Y. J.; Kang, H.; Han, J. W.; Noh, J. Self-Assembled Monolayers of Dioctyl Diselenides on Au(111). *Bull. Korean Chem. Soc.* **2008**, *29*, 1229−1232.
(36) de la Llave, E.; Scherlis, D. A. Selenium-Based Self-Assembled Monolayers: The Nature of Adsorbate-Surface Interactions. *Langmuir* **2010**, *26*, 173−178.
(37) Dishner, M. H.; Hemminger, J. C.; Feher, F. J. Scanning Tunneling Microscopy Characterization of Organoselenium Monolayers on Au(III). *Langmuir* **1997**, *13*, 4788−4790.
(38) Han, S. W.; Lee, S. J.; Kim, K. Self-Assembled Monolayers of Aromatic Thiol and Selenol on Silver: Comparative Study of Adsorptivity and Stability. *Langmuir* **2001**, *17*, 6981−6987.
(39) Huang, F. K.; Horton, R. C.; Myles, D. C.; Garrell, R. L. Selenolates as Alternatives to Thiolates for Self-Assembled Monolayers: A SERS Study. *Langmuir* **1998**, *14*, 4802−4808.
(40) Kafer, D.; Bashir, A.; Witte, G. Interplay of Anchoring and Ordering in Aromatic Self-Assembled Monolayers. *J. Phys. Chem. C* **2007**, *111*, 10546−10551.
(41) Samant, M. G.; Brown, C. A.; Gordon, J. G. Formation of an Ordered Self-Assembled Monolayer of Docosaneselenol on Gold(111). Structure by Surface X-Ray-Diffraction. *Langmuir* **1992**, *8*, 1615−1618.

(42) Sato, Y.; Mizutani, F. Formation and Characterization of Aromatic Selenol and Thiol Monolayers on Gold: In-Situ IR Studies and Electrochemical Measurements. *Phys. Chem. Chem. Phys.* **2004**, *6*, 1328−1331.
(43) Shaporenko, A.; Ulman, A.; Terfort, A.; Zharnikov, A. Self-Assembled Monolayers of Alkaneselenolates on (111) Gold and Silver. *J. Phys. Chem. B* **2005**, *109*, 3898−3906.
(44) Szelagowska-Kunstman, K.; Cyganik, P.; Schupbach, B.; Terfort, A. Relative Stability of Thiol and Selenol Based SAMs on Au(111) − Exchange Experiments. *Phys. Chem. Chem. Phys.* **2010**, *12*, 4400−4406.
(45) Weidner, T.; Shaporenko, A.; Ballav, N.; Ulman, A.; Zhamikov, M. Modification of Alkaneselenolate Monolayers by Low-Energy Electrons. *J. Phys. Chem. C* **2008**, *112*, 1191−1198.
(46) Yee, C. K.; Ulman, A.; Ruiz, J. D.; Parikh, A.; White, H.; Rafailovich, M. Alkyl Selenide- and Alkyl Thiolate-Functionalized Gold Nanoparticles: Chain Packing and Bond Nature. *Langmuir* **2003**, *19*, 9450−9458.
(47) Romashov, L. V.; Ananikov, V. P. Self-Assembled Selenium Monolayers: From Nanotechnology to Material Science and Adaptive Catalysis. *Chem.—Eur. J.* **2013**, *19*, 17640−17660.
(48) Jia, J. J.; Bendounan, A.; Kotresh, H. M. N.; Chaouchi, K.; Sirotti, F.; Sampath, S.; Esaulov, V. A. Selenium Adsorption on Au(111) and Ag(111) Surfaces: Adsorbed Selenium and Selenide Films. *J. Phys. Chem. C* **2013**, *117*, 9835−9842.
(49) Azzam, W. A Novel Method for Elimination of the Gold-Islands Formed in the Self-Assembled Monolayers of Benzeneselenol on Au(111) Surface. *Appl. Surf. Sci.* **2010**, *256*, 2299−2303.
(50) Nakano, K.; Sato, T.; Tazaki, M.; Takagi, M. Self-Assembled Monolayer Formation from Decaneselenol on Polycrystalline Gold as Characterized by Electrochemical Measurements, Quartz-Crystal Microbalance, XPS, and IR Spectroscopy. *Langmuir* **2000**, *16*, 2225−2229.
(51) Subramanian, S.; Sampath, S. Enhanced Stability of Short- and Long-Chain Diselenide Self-Assembled Monolayers on Gold Probed by Electrochemistry, Spectroscopy, and Microscopy. *J. Colloid Interface Sci.* **2007**, *312*, 413−424.
(52) Bain, C. D.; Troughton, E. B.; Tao, Y. T.; Evall, J.; Whitesides, G. M.; Nuzzo, R. G. Formation of Monolayer Films by the Spontaneous Assembly of Organic Thiols from Solution onto Gold. *J. Am. Chem. Soc.* **1989**, *111*, 321−335.
(53) Dishner, M. H.; Hemminger, J. C.; Feher, F. J. Direct Observation of Substrate Influence on Chemisorption of Methanethiol Adsorbed from the Gas Phase onto the Reconstructed Au(111) Surface. *Langmuir* **1997**, *13*, 2318−2322.
(54) Jung, C.; Dannenberger, O.; Xu, Y.; Buck, M.; Grunze, M. Self-Assembled Monolayers from Organosulfur Compounds: A Comparison between Sulfides, Disulfides, and Thiols. *Langmuir* **1998**, *14*, 1103−1107.
(55) Noh, J.; Jang, S.; Lee, D.; Shin, S.; Ko, Y. J.; Ito, E.; Joo, S. W. Abnormal Adsorption Behavior of Dimethyl Disulfide on Gold Surfaces. *Curr. Appl. Phys.* **2007**, *7*, 605−610.
(56) Cometto, F. P.; Macagno, V. A.; Paredes-Olivera, P.; Patrito, E. M.; Ascolani, H.; Zampieri, G. Decomposition of Methylthiolate Monolayers on Au(111) Prepared from Dimethyl Disulfide in Solution Phase. *J. Phys. Chem. C* **2010**, *114*, 10183−10194.
(57) Hayashi, T.; Morikawa, Y.; Nozoye, H. Adsorption State of Dimethyl Disulfide on Au(111): Evidence for Adsorption as Thiolate at the Bridge Site. *J. Chem. Phys.* **2001**, *114*, 7615−7621.
(58) Noh, J.; Hara, M. Nanoscopic Evidence for Dissociative Adsorption of Asymmetric Disulfide Self-Assembled Monolayers on Au(111). *Langmuir* **2000**, *16*, 2045−2048.
(59) Noh, J.; Murase, T.; Nakajima, K.; Lee, H.; Hara, M. Nanoscopic Investigation of the Self-Assembly Processes of Dialkyl Disulfides and Dialkyl Sulfides on Au(111). *J. Phys. Chem. B* **2000**, *104*, 7411−7416.
(60) Yang, G. H.; Liu, G. Y. New Insights for Self-Assembled Monolayers of Organothiols on Au(111) Revealed by Scanning Tunneling Microscopy. *J. Phys. Chem. B* **2003**, *107*, 8746−8759.
(61) Monnell, J. D.; Stapleton, J. J.; Jackiw, J. J.; Dunbar, T.; Reinerth, W. A.; Dirk, S. M.; Tour, J. M.; Allara, D. L.; Weiss, P. S. Ordered Local Domain Structures of Decaneselenolate and Dodecaneselenolate Monolayers on Au{111}. *J. Phys. Chem. B* **2004**, *108*, 9834−9841.
(62) Ishida, T.; Choi, N.; Mizutani, W.; Tokumoto, H.; Kojima, I.; Azehara, H.; Hokari, H.; Akiba, U.; Fujihira, M. High-Resolution X-Ray Photoelectron Spectra of Organosulfur Monolayers on Au(111): S(2p) Spectral Dependence on Molecular Species. *Langmuir* **1999**, *15*, 6799−6806.
(63) Kang, H.; Shin, D. G.; Han, J. W.; Ito, E.; Hara, M.; Noh, J. Unique Ordered Domains of Biphenylthiol Self-Assembled Monolayers on Au(111). *J. Nanosci. Nanotechnol.* **2012**, *12*, 557−562.
(64) Chesneau, F.; Zhao, J. L.; Shen, C.; Buck, M.; Zharnikov, M. Adsorption of Long-Chain Alkanethiols on Au(111): A Look from the Substrate by High Resolution X-Ray Photoelectron Spectroscopy. *J. Phys. Chem. C* **2010**, *114*, 7112−7119.
(65) Castner, D. G.; Hinds, K.; Grainger, D. W. X-Ray Photoelectron Spectroscopy Sulfur 2p Study of Organic Thiol and Disulfide Binding Interactions with Gold Surfaces. *Langmuir* **1996**, *12*, 5083−5086.
(66) Fonder, G.; Delhalle, J.; Mekhalif, Z. Exchange versus Intercalation of *n*-Dodecanethiol Monolayers on Copper in the Presence of *n*-Dodecaneselenol and vice versa. *Appl. Surf. Sci.* **2010**, *256*, 2968−2973.
(67) Kondoh, H.; Nakai, I.; Nambu, A.; Ohta, T.; Nakamura, T.; Kimura, R.; Matsumoto, M. Dissociative and Non-dissociative Adsorption of Selenophene on Au(111) Depending on the Preparation Method. *Chem. Phys. Lett.* **2001**, *350*, 466−472.
(68) Hayashi, T.; Wakamatsu, K.; Ito, E.; Hara, M. Effect of Steric Hindrance on Desorption Processes of Alkanethiols on Au(111). *J. Phys. Chem. C* **2009**, *113*, 18795−18799.
(69) Ito, E.; Ito, H.; Kang, H.; Hayashi, T.; Hara, M.; Noh, J. Influence of Surface Morphology and Substrate on Thermal Stability and Desorption Behavior of Octanethiol Self-Assembled Monolayers: Cu, Ag, and Au. *J. Phys. Chem. C* **2012**, *116*, 17586−17593.
(70) Kondoh, H.; Kodama, C.; Sumida, H.; Nozoye, H. Molecular Processes of Adsorption and Desorption of Alkanethiol Monolayers on Au(111). *J. Chem. Phys.* **1999**, *111*, 1175−1184.
(71) Lavrich, D. J.; Wetterer, S. M.; Bernasek, S. L.; Scoles, G. Physisorption and Chemisorption of Alkanethiols and Alkyl Sulfides on Au(111). *J. Phys. Chem. B* **1998**, *102*, 3456−3465.
(72) Nuzzo, R. G.; Zegarski, B. R.; Dubois, L. H. Fundamental-Studies of the Chemisorption of Organosulfur Compounds on Gold(111). Implications for Molecular Self-Assembly on Gold Surfaces. *J. Am. Chem. Soc.* **1987**, *109*, 733−740.
(73) Stettner, J.; Winkler, A. Characterization of Alkanethiol Self-Assembled Monolayers on Gold by Thermal Desorption Spectroscopy. *Langmuir* **2010**, *26*, 9659−9665.